# EVN, MERLIN, and VLA Observations of NRAO530

X. Y. Hong[1], J. H. Zhao[2], T. An[1], D. R. Jiang[1], W. H. Wang[1], W. X. Feng[1], and C. H. Sun[1]

[1]  Shanghai Astronomical Observatory, 80 Nandan Road, Shanghai 200030, China
[2]  Harvard-Smithsonian CfA, 60 Garden St, MS 78, Cambridge, MA 02138

**Abstract.** We present images of NRAO530 observed with the EVN (VLBI) at 5 GHz, the MERLIN at 1 .6 and 5 GHz, and the VLA at 5 and 8 GHz showing the complex morphology on scales from pc to kpc. The VLBI image shows a core-jet structure indicating a somehow oscillation trajectory on a scale of 30 mas, north to the strongest compact component (core). A core-jet structure extended to several hundreds mas at about P.A. $-50°$ and a distant component located 11 arcsec west to the core are detected in both the MERLIN and the VLA observations. An arched structure of significant emission between the core and the distant component is also revealed in both the MERLIN image at 1.6 cm and the VLA images at 8.4 and 5 GHz. The core component shows a flat spectrum with $\alpha \sim -0.02$ ($S \propto \nu^{-\alpha}$) while $\alpha \sim 0.8$ for the distant component. The steep spectrum of the distant component and the detection of the arched emission suggests that the western distant component is a lobe or a hot-spot powered by the nucleus of NRAO530. A patch of diffuse emission, 12 arcsec nearly east (P.A. 70°) to the core component, is also observed with the VLA at 5 GHz, suggesting a presence of a counter lobe in the source.

## 1. Introduction

The quasar NRAO530 is a well known optically violently variable (OVV) extragalactic source with $m_{pg} \sim 18.5$ mag (Whelch and Spinrad 1973) at a redshift of 0.902 (Junkkarinen 1984). It is an object of intensive observations at all wavelengths from radio to $\gamma$-ray. Weak polarization of the source was detected both at optical and radio bands. NRAO530 was detected by ROSAT with $1.84 \times 10^{-6}$ Jy at 1.3 keV (Brinkmann et al. 1994) and identified as a $\gamma$-ray source by the Energetic Gamma Ray Experiment Telescope (EGRET) with flux density of $4.6 \times 10^{-11}$ Jy at 2.55 GeV (Fichtel et al. 1994; Thompson et al. 1995). The detection of the source in high frequency indicates that the evidence for relativistic bulk motion of the emitting plasma exists in its nucleus. A Doppler factor of 5.2 of NRAO530 was estimated by assuming that the particles and magnetic field are in equipartition (Guuosa & Daly 1996).

NRAO530 has been extensively monitored as a low frequency variable source (e.g., Bondi et al. 1994). Three epochs early VLBI observations at 1.7 GHz showed the structure was oriented in north-south direction extended to 25 mas in P.A. $-7°$ (Romney et al. 1984, Bondi et al. 1994). The morphology of the maps shows two-sided structures. Its complex structure variations are not readily interpretable as angular expansion because the separation of components and the component sizes appear unchanged (Bondi et al. 1994).

Two epochs VLBI observations at 5 GHz showed a 4 mas slightly curved jet of the source towards to around the North direction, and no counter jet has been detected (Shen et al. 1997, and Hong et al. 1999). A jet-like feature extending approximately 5 mas from the core along P.A.$\sim 15°$ was seen on the VLBI image at 8.5 GHz by Tingay et al. (1998).

The source underwent a dramatic radio outburst in 1995 with amplitude higher than any found over 30 years of monitoring (Bower et al. 1997). The creation of new components in the jet associated with the outburst was revealed by their 86 GHz

VLBI observation with one component (C1, their notation) to a radio flare observed in mid of 1994 and another component (C2) to the 1995 outburst. The components moved to the southwest with apparent velocities of 7.4 and 7.9 $h^{-1}$ $c$, respectively, by assuming the brightest component as the core (Bower et al. 1997).

The 22 and 43 GHz VLBA monitoring of the source has been made during the flare in 1995 (5 epoch from 1994.45 to 1996.90) by Jorstad et al. (2001). Based on better time sampling, they interpreted the evolution by assuming the south component as the core and the brightness feature is the ejected component during the flare. This results shows the structure and motion are both oriented roughly to the north with apparent velocities in the range of 7 to 29 $h^{-1}$ $c$, with a stationary feature to the north at the distance of $\sim 1.4$ mas from the core (Jorstad et al. 2001).

VLA observation of the source at 1.4 GHz showed an unresolved core and a second unresolved component 11″ around in P.A. $-90°$ (Perley 1982) without evidence for a connection between the two (Romney et al. 1984).

In this paper, we focus on the extended radio emission of the source at the kpc scale and the relation between the pc and kpc structures with EVN (European VLBI Network), MERLIN, and VLA observations at multi-frequencies.

## 2. The observations and data reduction

A full-track 7-hour EVN + MERLIN observation (EH004) of the blazar NRAO530 was carried out at 5 GHz on February 19, 1997. The EVN array comprised Effelsberg, Shanghai, Cambridge, Jodrell Bank (Mark 2), Medicina, Noto, Onsala, Urumqi, WSRT, and Torun. The data were acquired with the Mk III VLBI recording system in Mode B with an effective bandwidth of 28 MHz and correlated at the Max-Plank Institut für Radioastronomie in Bonn. The EVN data were calibrated and fringe-fitted using the NRAO (Astronomical Image
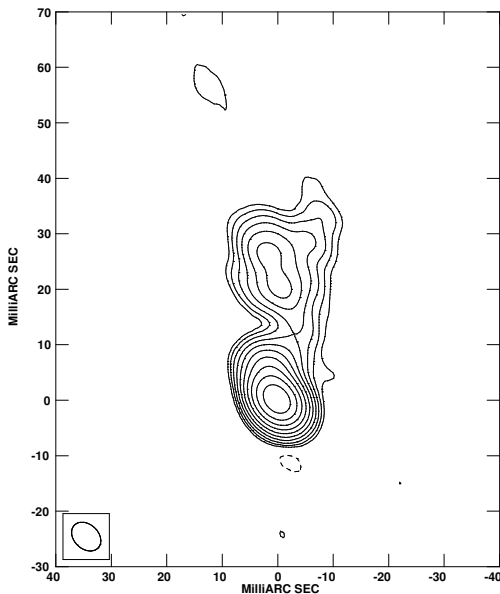
**Fig. 1.** EVN image of NRAO530 at 5 GHz. Peak flux density is 2.7 Jy/beam; the *r.m.s.* noise value is 0.5 mJy/beam; the lowest contours is 3 mJy/beam and contour levels increase by a factor of 2. FWHM: 5.9×4.4 mas; P.A. 46.6°

**Table 1.** Spectral index ($S \propto \nu^{-\alpha}$) of gaussian components

| Comp. | $\alpha^{5(MERLIN)}_{1.6(MERLIN)}$ | $\alpha^{8(VLA)}_{5(VLA)}$ | $\alpha^{8(VLA)}_{1.6(MERLIN)}$ | $\alpha^*$ |
|---|---|---|---|---|
| Core | 0.08 | −0.5 | −0.06 | −0.02 |
| West lobe | 1.0 | 1.0 | 0.8 | 0.8 |

note: $\alpha^*$ is calculated with least squares between 1.6 and 8 GHz.

Processing System) AIPS package. The initial amplitude calibration was accomplished using the system temperature measurements made during the observations and the priori station gain curves.

The MERLIN array of the EVN + MERLIN observation comprised 6 antennas (Defford, Cambridge, Knockin, Darnhall, Mark 2, and Tabley). The central frequency was 4.994 MHz and the observing bandwidth was 14 MHz.

An archive MERLIN data of NRAO530 at 1.6 GHz is available for our study. NRAO530 was observed as phase reference source with snapshot mode for total 2 hours on source with 46 scans over a period of 8 hours. The observation was carried out on May 8, 1998. The MERLIN array consists of 7 antennas (the same as above plus Lovell).

The quasar NRAO530 was observed with the VLA on Nov. 27, 1992 at 8.4 GHz and on June 17, 2003 (AZ143) at 4.8 GHz as a calibrator. The observations were carried out in snapshot mode. and used the standard VLA recording configuration (50 MHz bandwidth).

Post-processing including editing, phase and amplitude self-calibration, and imaging of the data were conducted in the AIPS package. Natural weighting was used for imaging to obtain the extended emission.

# 3. Results

## 3.1. VLBI image

The 5 GHz VLBI image displayed a jet to the North with a series of components on the scale of 30 mas with a somewhat oscillating trajectory (Fig. 1). The jet first moved in P.A. 15° for about 5 mas from the core, then turned sharply to the west and then the jet went to the North-East with the direction almost parallel to the first 5 mas jet. The low emission showed jet turned to the West again.

## 3.2. MERLIN images

To obtain the extended emission of the source, we tapered the 5 GHz MERLIN data at 1 mega-wavelengths with a comparable resolution of the MERLIN data at 1.6 GHz. The 5 GHz MERLIN image shows a core-jet structure in P.A. ∼ −50° on the scale of about 1″ and a distant component located at about 11″ west to the core. The west distant component extended in north-east to south-west direction and resolved into two components at resolution of 291 × 272 mas, −36.7°. No clear connection between the core and the west distant component was detected in the MERLIN observation (Fig. 2).

The 1.6 GHz MERLIN image shows a similar morphology to the 5 GHz MERLIN image. The core-jet structure and the west component are clearly detectable. Some week emission with an arch shape connecting between the core and the distant component has been detected in 1.6 GHz MERLIN observation (Fig. 3). This indicates that the west component is the lobe or hotspot of NRAO530.

## 3.3. VLA images

The VLA images at 8.1 and 4.8 GHz (Figs. 4&5) confirm the detection of the low emission between the core and the west distant component (let's call it the west lobe). Both images exhibit the same track, like a ballistic trajectory, from the core to the west lobe. This suggests that the emitting materials in the western lobe is powered by the nuclear source.

A patch of weak diffuse emission is detected in the region about 12.5″ nearly east (PA=70 °) to the core, which appears to be a counter lobe of the source. No clear connection between the east lobe and the core has been detected. However, the orientation of the milli-arcsec jet suggests that the lobe could be also powered by the nuclear source.

# 4. Conclusions and discussion

On the scale of parsec, NRAO530 appears to show that an oscillating jet consists of a number of emission components north to the core.

On the scale of kilo-parsec, the source exhibits a core jet structure in P. A. −50° and double lobe in the East-West direction. The west lobe is much stronger than the east lobe with the ratio about 5.5 in intensity. The core showed a flat spectral index ($\alpha = -0.02$, $S \propto \nu^{-\alpha}$), while the west lobe showed a steep spectral index ($\alpha = 0.8$). Fig. 6 shows the spectrum
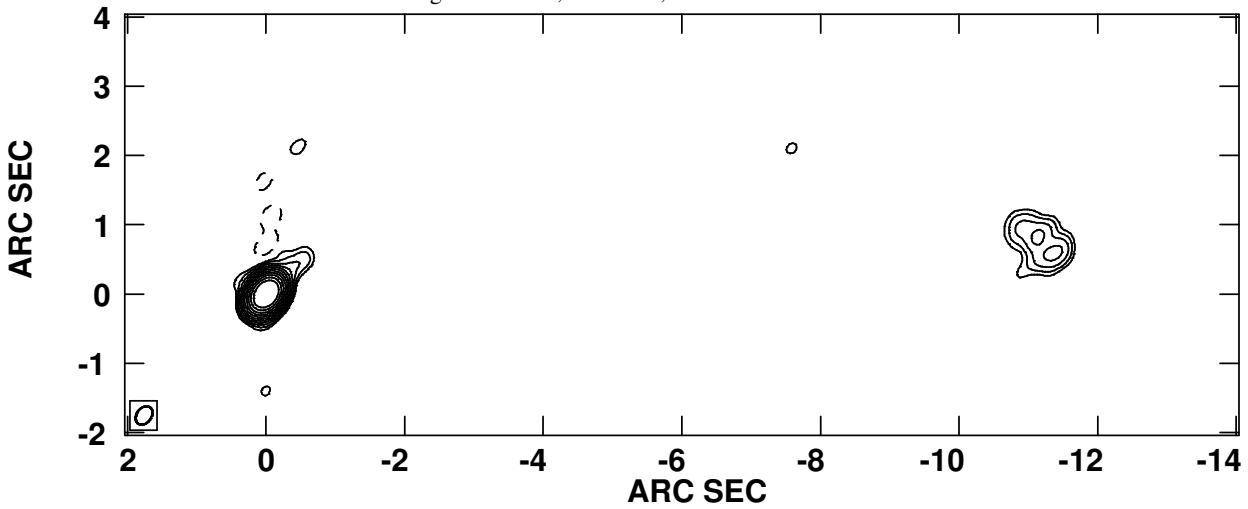
**Fig. 2.** A 5 GHz MERLIN image of NRAO530 at the epoch 1999.12, peak flux density= 4.55 Jy/beam, the r.m.s. noise is 0.2 mJy/beam, the lowest contour is 1.0 mJy/beam, contour levels increase by a factor of 2, FWHM: $0.29'' \times 0.27''$ ; P.A.$-36.7°$.
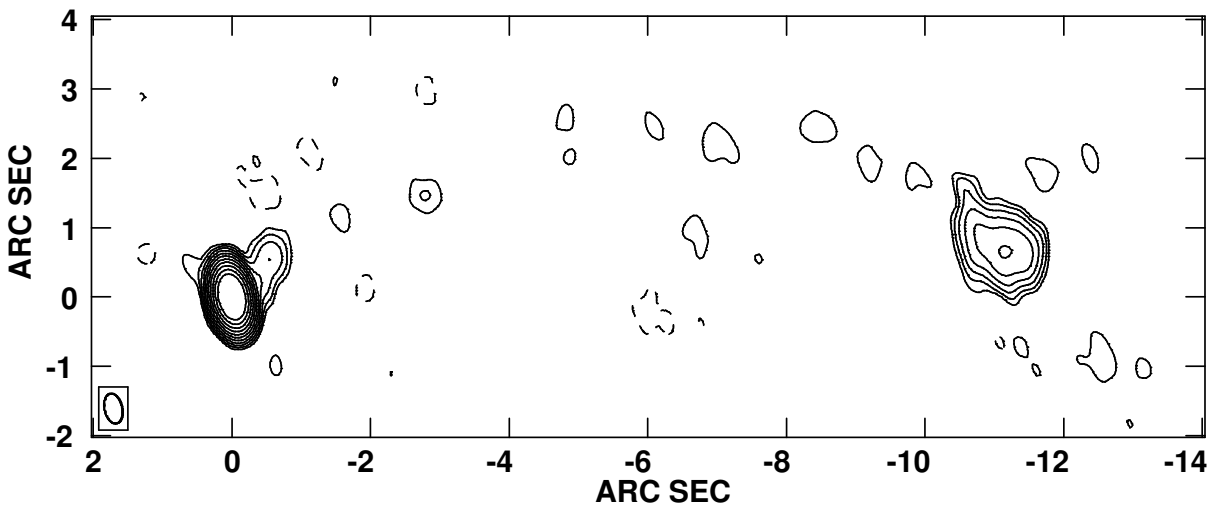


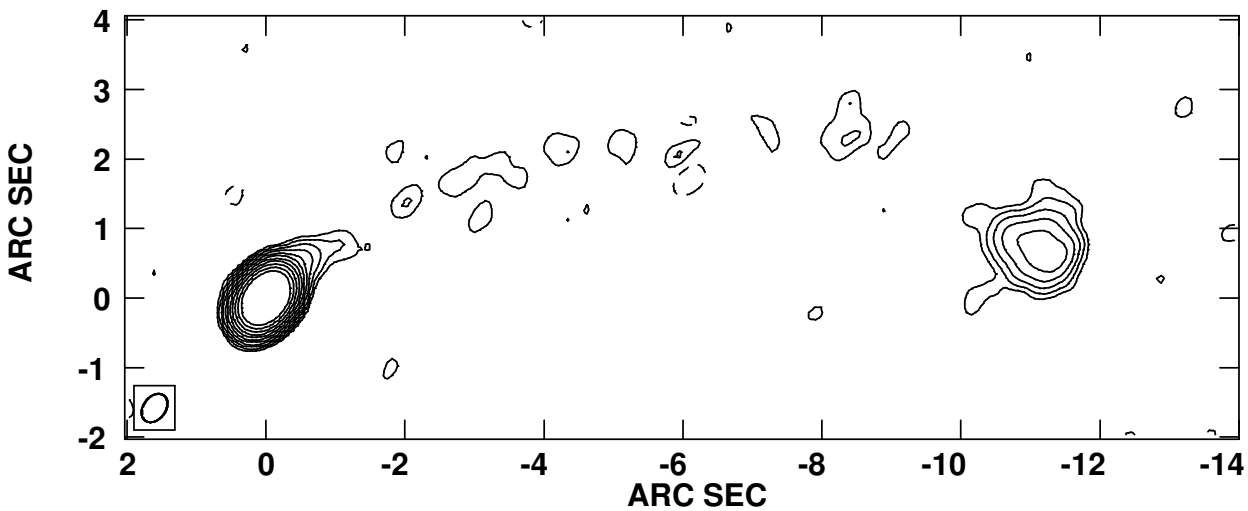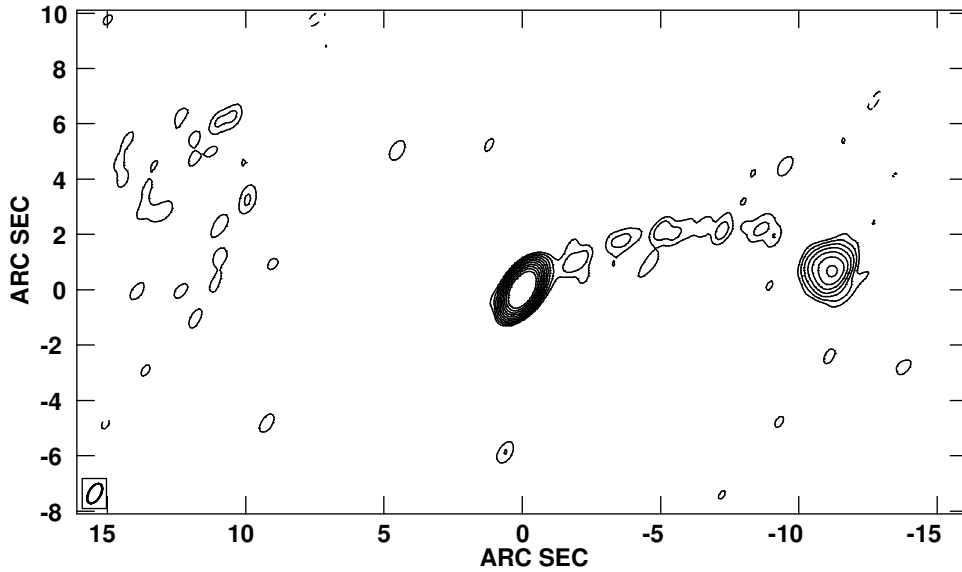**Fig. 3.** A 1.6 GHz MERLIN image of NRAO530 at the epoch 1998.35, peak flux density= 5.03 Jy/beam, the r.m.s. noise is 0.3 mJy/beam, the lowest contour is 1.0 mJy/beam, contour levels increase by a factor of 2, FWHM: $0.44'' \times 0.25''$; P.A. $12.1°$.



**Fig. 4.** A 8.15 GHz VLA image of NRAO530 at the epoch 1992.9, peak flux density= 5.58 Jy/beam, the r.m.s. noise is 0.15 mJy/beam, the lowest contour is 0.45 mJy/beam, contour levels increase by a factor of 2, FWHM: $0.45'' \times 0.32''$; P.A. $-36°$.

**Fig. 5.** A 5 GHz VLA image of NRAO530 at the epoch 2003, peak flux density= 4.38 Jy/beam, the r.m.s. noise is 0.15 mJy/beam, the lowest contour is 0.4 mJy/beam, contour levels increase by a factor of 2, FWHM: $0.79'' \times 0.43''$; P.A. $-29.9°$.
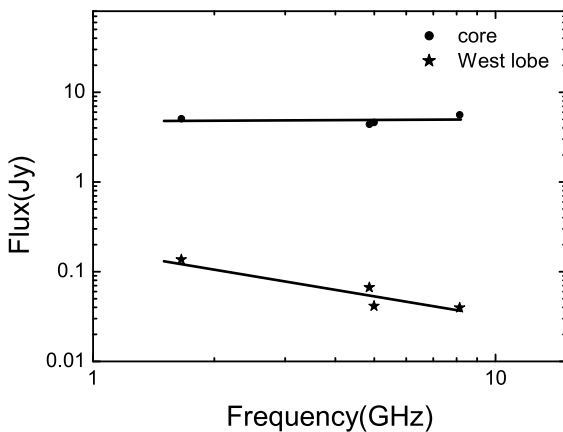


**Fig. 6.** The spectral indexes of the core and the west lobe.

of the core component and the west lobe with the four epochs MERLIN and VLA data. Table 1 gives the spectral indexes of the core component and the west lobe. A low emission are clear detected between the core component and the west lobe, while the connection between the core and the east lobe has not been detected.

It is not clear why the jet bents almost 90° from pc scale to kpc scale, which is not common for EGRET-detected AGNs (Hong et al. 1998). It may be caused by the interaction between the jets and the interstellar medium (IMS) of the host galaxy. It is also possible that the jet moves in a helical trajectory as 1156+295 (Hong et al. 2004).

## References

Bondi M., Padrielli L., Gregorini L. et al., 1994, A&A 287, 390
Bower G. C., Backer D. C., Wright M., Forster J. R., Aller H. D., and Aller M. F., 1997, ApJ, 484, 118
Brinkmann W., Siebert J., and Boller Th., 1994, A&A, 281, 355
Fichtel C. E., Bertsch D. L., Chiang J. et al., 1994, ApJS 94, 555
Guuosa A. and Daly R. A. 1996, ApJ 461, 600
Hong X. Y., Jiang D. R., and Shen Z. Q., 1998, A&A Letter, 330, L45
Hong X. Y., Venturi T., Wan T. S., Jiang D. R., Shen Z. Q., Liu X. et al. A&AS, 1999, 134, 201
Hong X. Y., Jiang D. R., Gurvits L. I., et al., A&A, 2004, 417, 887
Jorstad S. G., Marscher A. P., Mattox J. R., Wehrle A. E., Bloom S. D., and Yurchenko A. V., 2001, 134, 181
Junkkarinen V., 1984, PASP, 96, 539
Perley R. A., 1982, AJ 87, 859
Romney J., Padrielli L., Bartel N., Weiler K. W., Ficarra A., Mantovani F. et al., 1984, A&A 135,289
Shen Z. Q., Wan T. S., Moran J. M., Jauncey D. L., Reynolds J. E., Tziounis A. H. et al., 1997, AJ, 114, 1999
Thompson D. J., Bertsch D. L., Dingus B. L., Esposito J. A., Etienne A., Fichtel C. E. et al., 1995, ApJS, 101, 259
Tingay S. J., Murphy D. W., and Edwards P. G., 1998, ApJ. 500, 673
Whelch W. J. & Spinrad H., 1973, PASP, 85, 456